Optimum reference signal reconstruction for DVB-T based passive radars

Osama Mahfoudia*†, François Horlin† and Xavier Neyt *
Email: osama.mahfoudia@rma.ac.be francois.horlin@ulb.ac.be xavier.neyt@rma.ac.be
* Dept. CISS, Royal Military Academy, Brussels, Belgium
† Dept. OPERA, Université Libre de Bruxelles, Brussels, Belgium

***Abstract*—The present work investigates the optimum reconstruction of the reference signal for passive coherent location (PCL) radars exploiting Digital Video Broadcasting-Terrestrial (DVB-T) signals. Reference signal reconstruction is widely used to improve the signal-to-noise ratio (SNR) in the reference signal for DVB-T based PCL radars. Reference signal reconstruction is limited since for low SNR values, the signal demodulation is not sufficiently accurate which leads to a mismatch between the reconstructed signal and the transmitted one. In this work, we propose an optimum reconstruction strategy that includes an optimum estimation of the detected quadrature amplitude modulation (QAM) symbols, specific for radar applications. To verify the proposed detection strategy, we calculated analytic models for the optimum filter and the detection statistics. The analytic models are validated through Monte-Carlo simulations. The results show that the proposed method outperforms the conventional reference signal reconstruction scheme in terms of detection probability.**

I. Introduction

Passive coherent location (PCL) radars employ signals from non-cooperative transmitters, illuminators of opportunity (IOs), for target detection and tracking [1], [2]. The major advantages of the PCL radars are: low cost, interception immunity and ease of deployment. The IOs employed for PCL radar systems are transmitters for communication or broadcasting. For example, FM radio broadcast [3], digital audio and video broadcast (DAB and DVB-T) [4]–[10], and Global System for Mobile communications (GSM) base stations [11], [12]. The architecture of PCL radars in the bistatic configuration consists of two receiving channels: a reference channel (RC) and a surveillance channel (SC). The RC captures the direct-path signal from the IO and the SC receives the target echoes and interferences [13].

The detection in PCL radars can be performed with a cross-correlation (CC) detector. The CC detector cross-correlates the surveillance signal and a time-delayed and frequency-shifted copy of the reference signal [1]. The CC detector imitates the matched filter (MF) by employing the received reference signal instead of the exact transmitted signal.

The reference signal is often corrupted by noise which decreases the coherent integration gain for the CC detector and thus leads to a degradation of its performance in terms of detection probability compared to the MF. This issue has been addressed in [14] where an assessment of the impact of noise in the reference signal on the detection probability has been carried out employing theoretical analysis.

The PCL radars that exploit DVB-T signals can benefit from an enhancement of the reference signal SNR through a reconstruction of the received reference signal [13], [15], [16]. The reference signal reconstruction is supposed to provide a noise-free copy of the transmitted signal which increases the detection performance. In the reconstruction process, the received reference signal is demodulated and an estimate of the transmitted quadrature amplitude modulation (QAM) symbols is calculated via the QAM symbol detection. The noise-free signal is obtained by modulating the detected QAM symbols.

The correctness of the reconstructed reference signal depends on the QAM detection accuracy. An accurate QAM detection requires a relatively high SNR. For low SNR values, the QAM symbol detection error probability is high. Thus, the reconstructed signal (based on the detected QAM symbols) presents a mismatch with the transmitted one which leads to the degradation of the coherent integration gain. Therefore, the conventional approach of reference signal reconstruction performance is limited for low SNR scenarios.

The quantitative and theoretical aspects of the reference signal reconstruction approach are hardly studied in the literature. In this paper, we consider a DVB-T based PCL radar in the bistatic configuration. We neglect the effect of the direct-path and interference on the surveillance signal and we consider a noisy reference signal. We analyze the impact of the reference signal reconstruction on the CC detector performance and we propose an optimum reconstruction scheme that includes an optimum filtering of the detected QAM symbols. In addition, we introduce the use of a locally generated pilot subcarrier signal as a replacement for the noisy reference signal. In order to do so, we first present the reference signal model and the DVB-T signal structure. Then, we describe the reference signal reconstruction process and we analytically calculate the optimum filter for the detected QAM symbols. To verify the proposed strategy, we developed closed-form expressions for the detection statistics and validated them through Monte-Carlo (MC) simulations. The results have shown that the proposed strategy outperforms the conventional reference signal reconstruction approach.

This paper is organized as follows. Section 2 presents the received reference signal model and the DVB-T signal structure. Section 3 introduces the optimum filter design and calculation. Section 4 presents the detection statistics. In section 4, we present the numerical results. Section 5 concludes the paper.

II. Signal model

We consider a bistatic PCL radar exploiting the DVB-T signals as shown in figure 1 and we adopt the signal model employed in [14]. The reference signal $x_r(n)$ consists of a direct-path signal and a complex Gaussian thermal noise $v(n)$ with zero mean and a variance σ_v^2, i.e., $v(n) \sim \mathcal{CN}(0, \sigma_v^2)$. The reference signal can be expressed as

$$x_r(n) = \beta s(n) + v(n), \tag{1}$$

with β is a complex scaling parameter and $s(n)$ is the signal transmitted by the DVB-T broadcaster. The DVB-T signal follows a complex Gaussian distribution of zero mean and a variance σ_s^2, i.e., $s(n) \sim \mathcal{CN}(0, \sigma_s^2)$ [5].

The DVB-T standard employs the orthogonal frequency division multiplexing (OFDM) modulation scheme [17]. The DVB-T signal is structured into symbols and each DVB-T symbol is formed by K subcarriers. For one DVB-T symbol, the signal $s(n)$ is generated as follows

$$s(n) = \sum_{k=0}^{K-1} c_k e^{j2\pi f_k(n)}, \tag{2}$$

with K is the number of subcarriers, f_k is the frequency of the k^{th} subcarrier, and c_k are the complex-valued QAM symbols. Or, equivalently

$$\mathbf{s} = \mathbf{F}^{-1}\mathbf{c}, \tag{3}$$

with $\mathbf{F}$ is the DFT matrix of size $K \times K$ and $\mathbf{c}$ is the QAM symbol vector given by

$$\mathbf{c} = \left[c_0, c_1, c_2, \cdots, c_{K-1}\right]^T. \tag{4}$$

Figure 2 presents the structure of the DVB-T signal. The subcarriers are divided into three categories: data subcarriers, transmission parameter signalling (TPS) subcarriers, and pilot subcarriers. The data subcarriers transport video coded information. The TPS subcarriers carry transmission parameters such as channel coding and modulation type. The pilot subcarriers are transmitted at known frequencies and with known amplitudes, they are employed for signal synchronization and propagation channel estimation. If we neglect the TPS subcarriers, we can write

$$\mathbf{c} = \begin{pmatrix} \mathbf{c}_d \\ \mathbf{c}_p \end{pmatrix}, \tag{5}$$

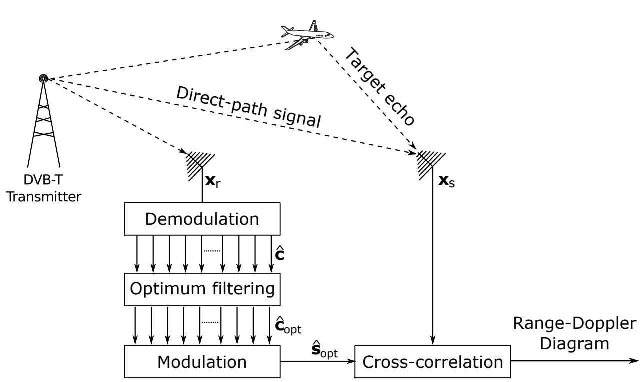

Fig. 1: The proposed detection scheme.

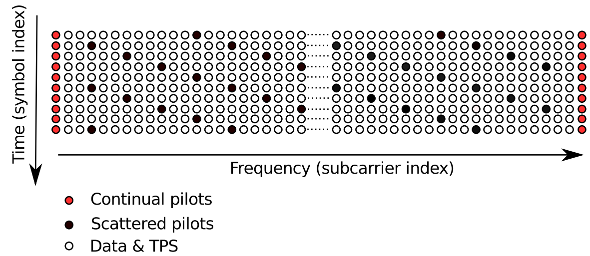

Fig. 2: DVB-T signal structure.

where $\mathbf{c}_d$ and $\mathbf{c}_p$ are the data subcarrier array and the pilot subcarrier array, respectively.

The pilot subcarriers are loaded with a pseudo-random binary sequence (PRBS). Let us call $p(n)$ the time-domain pilot signal which is the sum of the pilot subcarrier signals. Based on the central limit theorem (CLT), we can consider that $p(n)$ follows a complex Gaussian distribution with zero mean and a variance σ_p^2, i.e., $p(n) \sim \mathcal{CN}(0, \sigma_p^2)$. Similarly, we define the data signal $d(n)$ as the sum of data subcarrier signals. The data signal can be considered as Gaussian due to the randomness of the carried data and based on the CLT, i.e., $d(n) \sim \mathcal{CN}(0, \sigma_d^2)$. Therefore, we can write

$$s(n) = d(n) + p(n), \tag{6}$$

since $d(n)$ and $p(n)$ are statistically independent, we can write

$$\sigma_s^2 = \sigma_d^2 + \sigma_p^2, \tag{7}$$

and the ratio between the data signal and the pilot signal powers is defined as follows

$$\rho = \sigma_d^2 / \sigma_p^2, \tag{8}$$

the parameters σ_d^2, σ_p^2 and ρ are known for a given DVB-T transmission mode (2k or 8k).

An important parameter of the reference signal is the signal-to-noise ratio defined as

$$\mathrm{SNR_r} = |\beta|^2 \sigma_s^2 / \sigma_v^2, \tag{9}$$

an estimate of $\mathrm{SNR_r}$ can be calculated as follows [18]

$$\hat{\mathrm{SNR}}_\mathrm{r} = \frac{|\hat{\beta}|^2 \left(1+\rho\right) \sigma_p^2}{r_x - |\hat{\beta}|^2 \left(1+\rho\right) \sigma_p^2}, \tag{10}$$

where r_x is the power of the received signal calculated by

$$r_x = \mathrm{E}\left[x_r(n) x_r^*(n)\right], \tag{11}$$

and $\hat{\beta}$ is the estimate of the scaling parameter in equation (1) which is given by

$$\hat{\beta} = r_{xp} / \sigma_p^2, \tag{12}$$

with

$$r_{xp} = \mathrm{E}\left[x_r(n) p^*(n)\right]. \tag{13}$$

III. Optimum filter

The received reference signal is time and frequency synchronized for offset compensation. The synchronized signal is split into DVB-T symbols and the guard interval (GI) is removed from each symbol. For one DVB-T symbol, the demodulated signal is obtained by applying the following transformation

$$\mathbf{c}_r = \mathbf{F}\mathbf{x}_r, \tag{14}$$

with $\mathbf{F}$ is the DFT matrix and $\mathbf{x}_r$ is the synchronized reference signal after GI removal.

The QAM symbol detection of $\mathbf{c}_r$ leads to an estimate of the transmitted QAM symbols which we note $\hat{\mathbf{c}}$. The accuracy of data symbol detection depends on the $\mathrm{SNR_r}$, however, the pilot symbols can be generated locally since the PRBS is known at the receiver. Thus, the detected QAM symbols $\hat{\mathbf{c}}$ can be expressed as

$$\hat{\mathbf{c}} = \begin{pmatrix} \hat{\mathbf{c}}_d \\ \mathbf{c}_p \end{pmatrix}, \tag{15}$$

where $\hat{\mathbf{c}}_d$ represents the detected data QAM symbols. The data QAM symbols are detected with an error probability $\mathrm{P_e}$ which depends on the $\mathrm{SNR_r}$. The closed-form expression of $\mathrm{P_e}$ is given in [19].

The conventional approach for the reference signal reconstruction implies the use of the detected QAM symbols $\hat{\mathbf{c}}$ for the generation of the noise-free reference signal. This approach is efficient for negligible QAM symbol detection error, i.e., $\mathrm{P_e} \approx 0$. For low $\mathrm{SNR_r}$ values, $\mathrm{P_e}$ is significant. Thus, the reconstructed reference signal may present a mismatch with the transmitted one due to the wrongly estimated QAM symbols. To cope with this issue, we propose to optimally filter the detected QAM symbols. The optimum filter for the detected QAM symbols is obtained by minimizing the mean square symbol estimation error (MSE) that we note J. For each QAM symbol, we have

$$J = \mathrm{E}\left[|h\hat{c} - c|^2\right], \tag{16}$$

where h represents the filter weight, c is the exact QAM symbol and $\hat{c}$ is the estimated one. The optimum filter weights are calculated as follows [20]

$$h = \mathrm{E}\left[\hat{c}c^*\right]/\mathrm{E}\left[\hat{c}\hat{c}^*\right], \tag{17}$$

pilot subcarriers are reconstructed with no error which yields to $\hat{c}_p = c_p$, it follows that the filter weights for the pilot subcarriers are given by $h_p = 1$. While for data subcarriers, we have

$$\hat{c}_d = c_d \text{ with a probability of } (1 - \mathrm{P_e}), \tag{18}$$

since $\mathrm{E}\left[\hat{c}_d c_d^*\right] = 0$ for $\hat{c}_d \neq c_d$ [13], we can write

$$\mathrm{E}\left[\hat{c}_d c_d^*\right] = (1 - \mathrm{P_e})\mathrm{E}\left[\hat{c}_d \hat{c}_d^*\right], \tag{19}$$

hence, the filter weights for the data subcarriers are given by

$$h_d = (1 - \mathrm{P_e}), \tag{20}$$

thus, the optimally filtered QAM symbols can be expressed as

$$\hat{\mathbf{c}}_{\mathrm{opt}} = \begin{pmatrix} (1 - \mathrm{P_e})\hat{\mathbf{c}}_d \\ \mathbf{c}_p \end{pmatrix}. \tag{21}$$

We note $\hat{\mathbf{s}}_{\mathrm{opt}}$ the optimally reconstructed reference signal, it is obtained by

$$\hat{\mathbf{s}}_{\mathrm{opt}} = \mathbf{F}^{-1}\hat{\mathbf{c}}_{\mathrm{opt}}, \tag{22}$$

which can be written as

$$\hat{\mathbf{s}}_{\mathrm{opt}} = \mathbf{p} + (1 - \mathrm{P_e})\hat{\mathbf{d}}, \tag{23}$$

where $\hat{\mathbf{d}}$ is the data subcarrier signal and $\mathbf{p}$ is the pilot subcarrier signal.

IV. Detection statistics

The surveillance signal shall be detected using the following binary hypotheses

$$\begin{cases} \mathrm{H}_0: \; x_s(n) = w(n), \\ \mathrm{H}_1: \; x_s(n) = \alpha s(n-\tau)e^{j\omega_d n} + w(n), \end{cases} \tag{24}$$

under the null hypothesis (H_0), the surveillance signal is formed by a complex Gaussian thermal noise $w(n)$ of zero mean and a variance of σ_w^2, i.e., $w(n) \sim \mathcal{CN}(0, \sigma_w^2)$. In addition to the noise $w(n)$, the surveillance signal under the alternative hypothesis (H_1) contains a target echo time-delayed by τ, frequency-shifted by f_d with $\omega_d = 2\pi f_d$ and scaled by α. The complex parameter α is assumed to be constant during the integration time. The signal-to-noise ratio in the surveillance signal is given by

$$\mathrm{SNR_s} = |\alpha|^2\sigma_s^2/\sigma_w^2. \tag{25}$$

To retrieve the detection statistic expression, we consider a reconstructed reference signal with the following generalized expression

$$\hat{\mathbf{s}} = \mathbf{p} + a\hat{\mathbf{d}}, \tag{26}$$

with a is a constant parameter. The detection test is performed as follows

$$|\bar{T}|^2 = |\sum_{n=0}^{N-1} T_n|^2 \underset{\mathrm{H}_0}{\overset{\mathrm{H}_1}{\gtrless}} \lambda, \tag{27}$$

with λ is the detection threshold, N is the integration time and T_n for the range-Doppler cell (τ, f_d) is defined by

$$T_n = x_s(n)\hat{s}^*(n-\tau)e^{-j\omega_d n}, \tag{28}$$

under H_1, it yields

$$\begin{aligned} T_n = \; & \alpha\left(|p(n-\tau)|^2 + a\; d(n-\tau)\hat{d}^*(n-\tau)\right) \\ & + \alpha\left(a\; d(n-\tau)p^*(n-\tau) + \hat{d}^*(n-\tau)p(n-\tau)\right) \\ & + \left(a\; \hat{d}(n-\tau) + p(n-\tau)\right)^* w(n)e^{-j\omega_d n}, \end{aligned} \tag{29}$$

the mean of T_n under the alternative H_1 hypothesis can be expressed as

$$\mathrm{E}\left[T_n|\mathrm{H}_1\right] = \alpha\,\mathrm{E}\left[|p(n-\tau)|^2 + a\; d(n-\tau)\hat{d}^*(n-\tau)\right], \tag{30}$$

it follows that $\mathrm{E}\left[T_n|\mathrm{H}_1\right]$ will be of the form

$$\mathrm{E}\left[T_n|\mathrm{H}_1\right] = \alpha\,\left(\sigma_p^2 + a\;\epsilon\right), \tag{31}$$

with

$$\epsilon = \mathrm{E}\left[\hat{d}^*(n-\tau)d(n-\tau)\right]. \tag{32}$$

The quantity ϵ depends on the $\mathrm{SNR_r}$ value. According to (2), we can write

$$\epsilon = \mathrm{E}\left[\sum_{k_1=1}^{K_d}\sum_{k_2=1}^{K_d} c_{k_1}\hat{c}_{k_2}^{*} e^{j2\pi f_{k_1}(n-\tau)} e^{-j2\pi f_{k_2}(n-\tau)}\right], \quad (33)$$

where K_d is the number of the data subcarriers in one DVB-T symbol. Since the subcarriers are orthogonal we can write [13]

$$\mathrm{E}\left[c_{k_1}\hat{c}_{k_2}^{*} e^{j2\pi f_{k_1}(n-\tau)} e^{-j2\pi f_{k_2}(n-\tau)}\right]_{k_1\neq k_2} = 0, \quad (34)$$

hence, we get

$$\epsilon = \mathrm{E}\left[\sum_{k=1}^{K_d} c_k \hat{c}_k^{*}\right], \quad (35)$$

it follows that

$$\epsilon = K_d(1-\mathrm{P_e})\mathrm{E}\left[c_k c_k^{*}\right]. \quad (36)$$

The variance of the data signal $d(n)$ can be defined by

$$\sigma_d^2 = K_d \mathrm{E}\left[c_k c_k^{*}\right], \quad (37)$$

therefore, the quantity ϵ can be expressed as

$$\epsilon = (1-\mathrm{P_e})\sigma_d^2, \quad (38)$$

finally, the mean of T_n under $\mathrm{H_1}$ is given by

$$\mathrm{E}\left[T_n|\mathrm{H_1}\right] = \alpha\left(\sigma_p^2 + a(1-\mathrm{P_e})\sigma_d^2\right), \quad (39)$$

similarly, we can find that the variance of T_n under $\mathrm{H_1}$ is expressed as

$$\begin{aligned}\mathrm{var}\left[T_n|\mathrm{H_1}\right] = &\ |\alpha|^2\left(\sigma_p^4 + a^2(1-\mathrm{P_e})^2\sigma_d^4\right)\\ &+ |\alpha|^2\left(a^2 + 2a(1-\mathrm{P_e}) + 1\right)\sigma_d^2\sigma_p^2\\ &+ \left(\sigma_p^2 + a^2\sigma_d^2\right)\sigma_w^2, \end{aligned} \quad (40)$$

note that the mean and variance of T_n under the null hypothesis are obtained by setting $\alpha = 0$ in the equations (39) and (40), respectively.

The detection statistic $\bar{T}$ is calculated as follows

$$\bar{T} = \sum_{n=0}^{N-1} T_n, \quad (41)$$

Since the samples of T_n are statistically independent and due to the CLT, we can assume that the statistic $\bar{T}$ follows a complex Gaussian distribution with parameters (μ_0, σ_0^2) under $\mathrm{H_0}$ and (μ_1, σ_1^2) under $\mathrm{H_1}$. Those parameters are calculated as follows

$$\mu_0 = N\,\mathrm{E}\left[T_n|\mathrm{H_0}\right], \quad (42)$$

$$\mu_1 = N\,\mathrm{E}\left[T_n|\mathrm{H_1}\right], \quad (43)$$

$$\sigma_0^2 = N\,\mathrm{var}\left[T_n|\mathrm{H_0}\right], \quad (44)$$

$$\sigma_1^2 = N\,\mathrm{var}\left[T_n|\mathrm{H_1}\right], \quad (45)$$

the false alarm probability $\mathrm{P_{FA}}$ and the detection probability $\mathrm{P_D}$ can be calculated based on the retrieved parameters μ_0, μ_1, σ_0^2 and σ_1^2 [14].

To obtain the detection statistic parameters for the scenario where the conventional reconstruction is employed, we set $a = 1$. In the same way, we can get those parameters for the case of using a locally generated pilot-only signal as a reference signal by setting $a = 0$. Similarly, for the optimum reconstructed signal, we set $a = (1-\mathrm{P_e})$. For the noisy reference signal, the detection statistic parameters are defined in [14].

V. Numerical results

To validate the retrieved expressions and the proposed approach, we carried out Monte-Carlo simulations for a number of trials $N_{trials} = 10^6$. The false-alarm probability was fixed at $\mathrm{P_{FA}} = 10^{-4}$ with an integration time of $N = 10^5$ and a signal-to-noise ratio in the surveillance signal of $\mathrm{SNR_s} = -32$ dB.

Figure 3 shows the MC and theoretical results for four detection schemes represented by four reference signal variants: a noisy reference signal (without reconstruction), a non-filtered reconstructed reference signal, a reference signal formed by pilot signal, and an optimum reference signal (reconstructed and filtered). We notice that the MC simulation results fit perfectly with the theoretical ones which validates the theoretical analysis and the retrieved expressions.

As expected, the reference signal reconstruction improves the detection probability. This improvement is due to the $\mathrm{SNR_r}$ enhancement in the reconstructed reference signal. For low $\mathrm{SNR_r}$ values, the efficiency of the conventional reconstruction is limited since the QAM detection error is considerable.

For the detection scheme that employs the pilot signal only, the detection probability is constant as a function of the $\mathrm{SNR_r}$ values since the reference signal is locally generated. For $\mathrm{SNR_r} < -10$ dB, employing a pilot-only reference signal outperforms the use of the conventionally reconstructed reference signal. In fact, for that range of $\mathrm{SNR_r}$ values, the reconstruction noise (due to the QAM estimation error) is higher than the loss due to using only the pilot signal for detection.

The detection scheme that employs the optimally filtered signal surpasses the other methods. For $\mathrm{SNR_r} > -20$ dB, the designed optimum filter controls the contribution of the data subcarriers in the reference signal according to the QAM detection probability $\mathrm{P_e}$. Note that the parameter $(1-\mathrm{P_e})$ that regulates the filter behavior is directly proportional to the $\mathrm{SNR_r}$ which explains the results for the considered $\mathrm{SNR_r}$

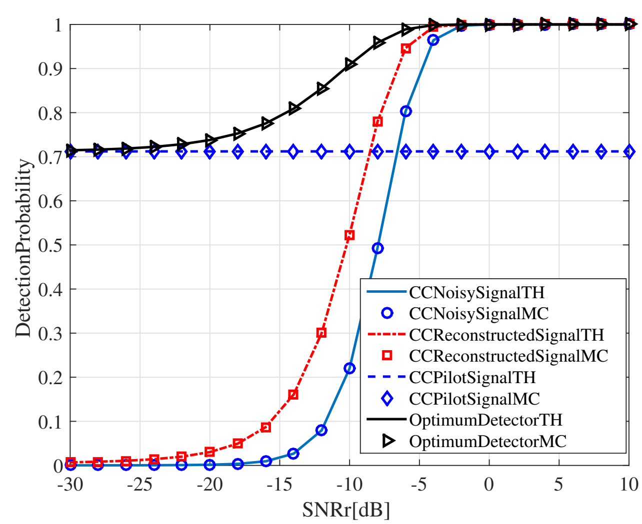

Fig. 3: Detection probability as function of $\mathrm{SNR_r}$ with an integration time of 10^5, $\mathrm{SNR_s} = -32$ dB and $\mathrm{P_{FA}} = 10^{-4}$, MC: Monte-Carlo results and TH: theoritical results.

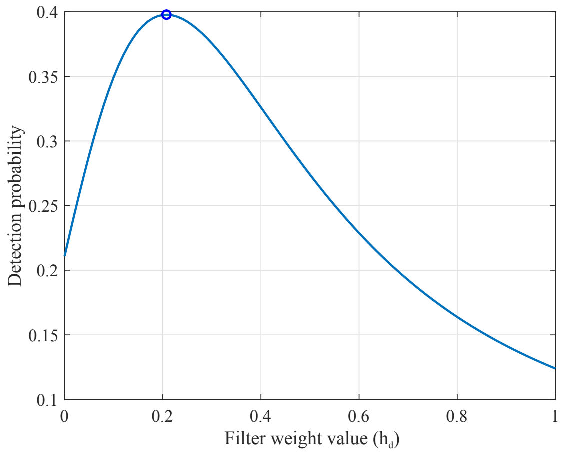

Fig. 4: Detection probability as function of the filter weight for an integration time of 10^5, $\mathrm{SNR_r} = -10$ dB, $\mathrm{SNR_s} = -35$ dB and $\mathrm{P_{FA}} = 10^{-4}$.

value range. For $\mathrm{SNR_r} < -20$ dB, the QAM detection error probability tends to 1, consequently, the optimum filter disables the use of data subcarrier signal and the resulting reference signal is exclusively formed by the pilot signal.

Figure 4 presents the detection probability as a function of the filter weight (the constant a of the equation (26)) with an integration time of $N = 10^5$, $\mathrm{SNR_r} = -10$ dB, $\mathrm{SNR_s} = -35$ dB, and $\mathrm{P_{FA}} = 10^{-4}$. In this case, the calculated optimum value of a is $a_{\mathrm{opt}} = 1 - \mathrm{P_e} = 0.21$ which is the value that maximizes the detection probability in figure 4. Thus, the proposed method for reference signal reconstruction maximizes the detection probability compared to other reconstruction schemes.

VI. Conclusion

In this paper, we provided an analytic assessment of the reference signal reconstruction for DVB-T based PCL radars and we proposed an optimum reconstruction scheme specific for radar applications. In addition, the use of pilot signal for detection has been investigated and validated. The proposed approach of filtering the detected QAM symbols outperforms the conventional reconstruction method, and extends the applicability of the reference signal reconstruction technique for low SNR values. In our future work, we will apply the proposed detection scheme on real measurements and we will consider the case where the interference in the surveillance signal is significant. Also, we will analyze the impact of the QAM symbols decoding to the bit-level on the detection performance.

References

[1] H. D. Griffiths and C. J. Baker, "Passive coherent location radar systems. Part 1: Performance prediction," *IEE Proceedings - Radar, Sonar and Navigation*, vol. 152, no. 3, p. 153, 2005.

[2] C. J. Baker, H. D. Griffiths, and I. Papoutsis, "Passive coherent location radar systems. Part 2: Waveform properties," *IEE Proceedings - Radar, Sonar and Navigation*, vol. 152, no. 3, p. 160, 2005.

[3] S. Bayat, M. M. Nayebi, and Y. Norouzi, "Target detection by passive coherent FM based bistatic radar," in *Radar, 2008 International Conference on*, pp. 412–415, sep 2008.

[4] C. R. Berger, B. Demissie, J. Heckenbach, P. Willett, and S. Zhou, "Signal Processing for Passive Radar Using OFDM Waveforms," *Selected Topics in Signal Processing, IEEE Journal of*, vol. 4, no. 1, pp. 226–238, 2010.

[5] K. Pölönen and V. Koivunen, "Detection of DVB-T2 control symbols in passive radar systems," in *Sensor Array and Multichannel Signal Processing Workshop (SAM), 2012 IEEE 7th*, pp. 309–312, 2012.

[6] M. Conti, F. Berizzi, M. Martorella, E. D. Mese, D. Petri, and A. Capria, "High range resolution multichannel DVB-T passive radar," *IEEE Aerospace and Electronic Systems Magazine*, vol. 27, pp. 37–42, oct 2012.

[7] M. Ummenhofer, J. Schell, J. Heckenbach, H. Kuschel, and D. W. D'O Hagan, "Doppler estimation for DVB-T based Passive Radar systems on moving maritime platforms," in *2015 IEEE Radar Conference (RadarCon)*, pp. 1687–1691, IEEE, may 2015.

[8] R. Tao, H. Z. Wu, and T. Shan, "Direct-path suppression by spatial filtering in digital television terrestrial broadcasting-based passive radar," *IET Radar, Sonar Navigation*, vol. 4, no. 6, pp. 791–805, 2010.

[9] F. Berizzi, M. Martorella, D. Petri, M. Conti, and A. Capria, "USRP technology for multiband passive radar," in *2010 IEEE Radar Conference*, pp. 225–229, 2010.

[10] D. Langellotti, F. Colone, P. Lombardo, E. Tilli, M. Sedehi, and A. Farina, "Over the Horizon maritime surveillance capability of DVB-T based passive radar," in *Microwave Conference (EuMC), 2014 44th European*, pp. 1812–1815, oct 2014.

[11] X. Neyt, J. Raout, M. Kubica, V. Kubica, S. Roques, M. Acheroy, and J. G. Verly, "Feasibility of STAP for passive GSM-based radar," in *Radar, 2006 IEEE Conference on*, pp. 6 pp.–, 2006.

[12] M. Kubica, V. Kubica, X. Neyt, J. Raout, S. Roques, and M. Acheroy, "Optimum target detection using illuminators of opportunity," in *Radar, 2006 IEEE Conference on*, pp. 8 pp.–, 2006.

[13] J. E. Palmer, H. A. Harms, S. J. Searle, and L. M. Davis, "DVB-T Passive Radar Signal Processing," *IEEE Transactions on Signal Processing*, vol. 61, pp. 2116–2126, apr 2013.

[14] J. Liu, H. Li, and B. Himed, "Analysis of cross-correlation detector for passive radar applications," in *Radar Conference (RadarCon), 2015 IEEE*, pp. 772–776, 2015.

[15] S. Searle, S. Howard, and J. Palmer, "Remodulation of DVB-T signals for use in Passive Bistatic Radar," in *Signals, Systems and Computers (ASILOMAR), 2010 Conference Record of the Forty Fourth Asilomar Conference on*, pp. 1112–1116, nov 2010.

[16] M. K. Baczyk and M. Malanowski, "Decoding and reconstruction of reference DVB-T signal in passive radar systems," in *Radar Symposium (IRS), 2010 11th International*, pp. 1–4, 2010.

[17] EBU/ETSI JTC, "Digital Video Broadcasting (DVB);Framing structure, channel coding and modulation for digital terrestrial television," tech. rep., Stadard, 2004.

[18] A. Y. Gafer, S. Elsadig, and J. Varun, "Front-end signal to noise ratio estimation for DVBT fixed reception in flat-fading channel," in *Intelligent and Advanced Systems (ICIAS), 2012 4th International Conference on*, vol. 1, pp. 296–300, 2012.

[19] J. R. Barry, E. A. Lee, D. G. Messerschmitt, and E. A. Lee, *Digital communication*. Springer, 2004.

[20] S. Haykin, *Adaptive Filter Theory (3rd Ed.)*. Upper Saddle River, NJ, USA: Prentice-Hall, Inc., 1996.